Progress In Electromagnetics Research C, Vol. 42, 177–190, 2013

WIDEBAND DGS CIRCULAR RING MICROSTRIP ANTENNA DESIGN USING FUZZY APPROACH WITH SUPPRESSED CROSS-POLAR RADIATIONS

Rakesh Sharma*, Abhishek Kandwal, and Sunil Kumar Khah

Electromagnetic Analysis Lab, Department of Physics and Materials Science, Jaypee University of Information Technology, Waknaghat, Solan 173234 (H.P), India

Abstract—This paper presents a novel design of a circular ring defected ground structure (DGS) antenna for bandwidth enhancement using fuzzy logic approach. The ground plane of the antenna is defected by introducing circular ring sector type of defect beneath the circular ring patch. The position of the defect in the ground plane to attain the highest return loss and corresponding frequency is determined by using Fuzzy Inference System (FIS). The antenna resonates in X-band showing wideband characteristics with improved gain and reduced cross polar components. The return loss and analogous frequency obtained from simulated results and fuzzy system are compared and are in good agreement. The return loss and input impedance is measured experimentally and compared with the simulated results. Parameters like impedance bandwidth, VSWR and antenna gain are likewise calculated and discussed. The simulated results for the radiation pattern of the proposed design with polarization (Co-polar and Cross-polar) are also presented. The simulated impedance bandwidth of about 1.33 GHz (1.2 GHz experimentally) in X-band is obtained with a gain of 6.43 dB and also cross-polarized radiations have an isolation of 20 dB.

1. INTRODUCTION

Microstrip patch antennas have found widespread applications especially in wireless communication systems primarily due to their simplicity, conformability, low manufacturing cost, light weight,

Received 15 June 2013, Accepted 31 July 2013, Scheduled 2 August 2013

* Corresponding author: Rakesh Sharma (str.phy@gmail.com).

low profile, reproducibility, reliability, and ease in fabrication and integration with solid-state devices [1–6]. However, microstrip antennas have some disadvantages also. One disadvantage is the excitation of surface waves in the substrate layer. Surface waves are undesired because when a patch antenna radiates, a portion of total available radiated power becomes trapped along the surface of the substrate. It can extract total available power for radiation to space wave. Therefore, surface wave can reduce the antenna efficiency, gain and bandwidth. In general, the bandwidth of simple patch antenna geometries of regular shape is very poor (1 to 2%) and their gain is also very low [7–9]. With recent advancements in the communication systems, the demand of multi-band antennas with enhanced bandwidth was realized. The use of defected ground microstrip antennas in electromagnetic radiations has been a recent topic of interest in the world. The microstrip antennas can show wide-band characteristics while introducing defects in the ground plane. Recently, there has been an increasing interest in the applications of defected ground structure (DGS) in microwave and millimeter wave applications. DGS is realized by etching a defected pattern in the ground plane, this etched pattern interferes with the shield current distribution in the ground plane which affects the characteristics of the antenna. This disturbance creates beneficial capacitance and inductance effect on the structure. It affects the input impedance and provides band rejection characteristics from the resonance property. It can also control the excitation and the electromagnetic waves propagating through the substrate layers, which results in slow wave effect of radiation [10–13].

Many shapes of DGS have been studied such as concentric ring, circle, spiral, dumbbells, elliptical and U- and V-slots. Each DGS shape can be represented as an equivalent circuit consisting of inductance and capacitance, which leads to a certain frequency band gap determined by the shape, dimension and position of the defect. DGS gives an extra degree of freedom in microwave circuit design and can be used for a wide range of applications. Several types of slots and defects are trenched in the ground ofthe microstrip antenna so that the size could be reduced and impedance bandwidth and gain can be enhanced [14–20]. The DGSs have been successively introduced to control and improve the radiation properties of the microstrip antennas. The defects introduced in the ground plane leads to the suppression of the cross-polarized radiations, reduction of the mutual coupling between the microstrip array elements and elimination of scan blindness of microstrip phased arrays [21–27].

This paper discusses the influence of circular ring sector shape DGS towards the improvement of the radiation properties. By

adding the DGS, therefore, will suppress surface wave propagation in the dielectric layer, which affects the resonance properties of the structure. The Fuzzy Inference System (FIS) is deployed to obtain the optimized position of the defect to have the highest return loss. The antenna structures without and with defected ground plane are therefore presented and compared. The properties such as return loss, input impedance are simulated and experimentally measured. The impedance bandwidth, voltage standing wave ratio (VSWR) is thus calculated. Radiation characteristics such as antenna gain, side lobe level, and back radiation are thus discussed. The proposed antenna design is analyzed by simulation software Ansoft HFSS and the experimental verification is carried out using R & S ZVL Vector Network Analyzer.

2. THEORY

A circular ring microstrip antenna comprises a ring shaped conductor on one side of the substrate and a metal ground plane on the other side. For a circular ring antenna, the cavity model provides the general solution of the wave equation

$$\begin{aligned} \left(\nabla^2 + k^2\right)\vec{E} &= 0 \\ k &= \frac{2\pi\sqrt{\epsilon_r}}{\lambda_0} \end{aligned} \tag{1}$$

in cylindrical coordinates is given as [7]:

$$\begin{aligned} E_z &= E_0[J_n(k\rho)Y_n'(ka) - J_n'(ka)Y_n(k\rho)]\cos n\phi \\ H_\rho &= \frac{j}{\omega\mu\rho}\frac{\partial E_z}{\partial\phi}, \quad H_\phi = \frac{-j}{\omega\mu}\frac{\partial E_z}{\partial\rho} \end{aligned} \tag{2}$$

where $J_n(\cdot)$ and $Y_n(\cdot)$ are the Bessel functions of first and second kind of order n, and a is the inner radius of the ring respectively. The other field components are zero inside the cavity. The surface current on the lower surface of the ring metallization is given by

$$\vec{J_s} = -\hat{z}X\vec{H} = -\hat{\phi}H_\rho + \hat{\rho}H_\phi$$

Or

$$\begin{aligned} J_\phi &= \frac{jnE_0}{\omega\mu\rho}[J_n(k\rho)Y_n'(ka) - J_n'(ka)Y_n(k\rho)]\sin n\phi \\ J_\rho &= -\frac{jkE_0}{\omega\mu}[J_n'(k\rho)Y_n'(ka) - J_n'(ka)Y_n'(k\rho)]\cos n\phi \end{aligned} \tag{3}$$

The radial component of the surface current must vanish along the edges at the $\rho = a$ and $\rho = b$ to satisfy the magnetic wall boundary conditions. This leads to

$$J_\rho(\rho = a, b) = H_\phi(\rho = a, b) = 0 \tag{4}$$

where a and b are the inner and outer radii of the circular ring antenna.

Application of this boundary condition leads to the well-known characteristic equation for the resonant modes

$$J'_n(kb)Y'_n(ka) - J'_n(ka)Y'_n(kb) = 0 \tag{5}$$

For the given values of a, b, ϵ_r and n, the frequency is varied and the roots of (5) are determined. If we denote these roots by k_{nm} for the resonant T_{nm} modes and form X_{nm} such that $X_{nm} = k_{nm}a$. The integer n denotes the azimuthal variation as per $\cos n\phi$, while the integer m represents the mth zero of (5) and denotes the variation of fields across the width of the ring.

The resonant frequency of the circular ring antenna is obtained by setting

$$k_{nm} = \frac{X_{nm}}{a}, \quad f_{nm} = \frac{X_{nm}c}{2\pi a\sqrt{\epsilon_{re}}} \tag{6}$$

where c is the velocity of light in space, ϵ_{re} is the effective dielectric constant respectively.

3. ANTENNA DESIGN AND FUZZY APPROACH (FIS)

The results of the development design of a compact wideband defected ground antenna using Fuzzy approach for use in communication applications are presented in this section. Bandwidth is specified as the frequency bandwidth in which the return loss is above 10 dB.

3.1. Geometry

In the present communication, the outer radius is three times the inner radius ($b = 3a$) of the proposed ring antenna. The design consists of a circular ring microstrip antenna with a defected ground shown in Figure 1. Figures 1(a) and 1(b) show the top and bottom views of the antenna with purported defect respectively. The circular patch antenna with DGS is designed on a commercially available FR-4 substrate of dielectric constant 4.3 and height 1.59 mm respectively. A circular annular ring of inner radius, $a = 5$ mm and outer radius, $b = 15$ mm is printed over the substrate material. The ground plane of 50 mm $\times$ 50 mm is defected by introducing four circular ring sectors. The angular width of each sector is selected to be 75° about the center

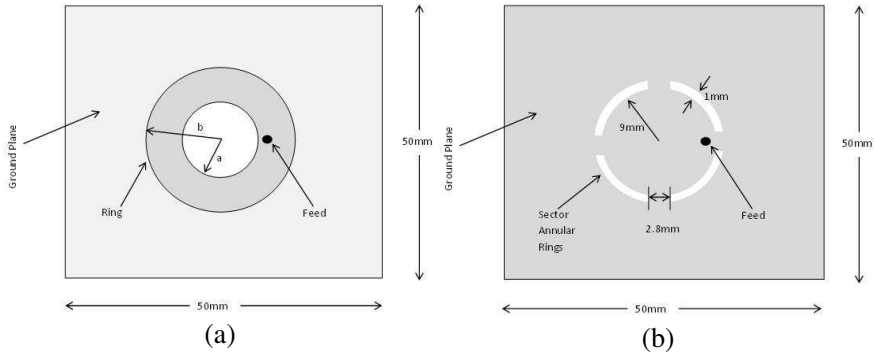

Figure 1. Design of defected ground circular patch microstrip antenna. (a) Top view, (b) bottom view.

of the ground plane. A gap of 15° about the center is present between the two adjacent ring sectors. The antenna is fed by a coaxial probe at 7 mm from the center of the ring. The configuration for the circular ring microstrip antenna without defected ground is same as for defected ground antenna except for the ground plane. The each ring sector has 9 mm and 10 mm as inner and outer radii respectively. These values for the position of the defect are obtained from the FIS model optimization which is discussed in the next section.

3.2. Fuzzy Inference System (FIS) Model

A new modeling approach by using fuzzy inference system (FIS) for computing various parameters of the microstrip antenna like input impedance, resonant frequency and back scattering response has been studied earlier [28–30]. The fuzzy inference system (FIS) is a popular computing structure based on the concept of fuzzy set theory, fuzzy if-then rules, and fuzzy reasoning. With crisp inputs and outputs, a fuzzy inference system implements a nonlinear mapping from its input space to output space. The Matlab Fuzzy Logic Toolbox was used for FIS development [31].

In the present study, FIS model is used to optimize the position of the defect in the ground plane so as to obtain the highest return loss in X-band. The Mamdani fuzzy inference system is used for the optimization purpose. The inputs to the FIS system are feed position, substrate and position of the defect in the ground plane. The input parameter values are the crisp numbers obtained from a data set generated from simulations carried out for the proposed antenna using CST Studio Suite. The feed point location is 7 mm, substrate used is

FR-4 having $\epsilon_r = 4.3$ and the outer radius of the defect (circular ring sectors) is varied from 6 mm to 19.5 mm with a step height of 1.5 mm respectively. The width of the defect is kept constant (i.e., 1 mm) during the entire variation. The output of the FIS model represents the return loss and operating frequency parameters of the proposed antenna. The return loss ranges from 0 to 30 dB and frequency lies in the X-band.

The results obtained from the fuzzy model are compared with the simulated results from Ansoft HFSS software and are shown in Table 1 (for test data). From the results, it is clear that outcomes for frequency and return loss are in good agreement with each other with a marginal difference. The position of the defect with minimum return loss comes at 10 mm (at the 3rd row in Table 1) for both simulated and FIS model results. Hence, this optimized value is used for the outer radius of the defect for both simulation and experimental design of the antenna. The surface plots for the variation of frequency and return loss with feed location and defect position are shown in Figure 2.

Table 1. Comparison of simulated results (HFSS) and FIS model.

Sr. No.	Position of Defect (in mm)	Simulated Results (HFSS)		FIS Model	
		Frequency (GHz)	Return Loss (dB)	Frequency (GHz)	Return Loss (dB)
1.	9.8	11.2997	16.3309	11.3	17.1
2.	9.9	11.4396	22.7070	11.3	18.2
3.	**10**	**11.2918**	**25.6347**	**11.3**	**24.1**
4.	10.1	11.1227	22.6383	11.1	23
5.	10.2	11.0544	20.1780	11.1	20.7
6.	10.3	11.1211	15.9104	11.1	15.3
7.	10.4	11.1544	13.7171	11.2	13.2
8.	10.5	11.1644	12.4568	11.2	13

3.3. Prototype of the Proposed Structure

The parameters like return loss, input impedance, bandwidth, gain and radiation patterns and VSWR are studied for the proposed geometry by using commercially available Ansoft HFSS simulation software. For the experimental verification of the simulated results, the prototype of the proposed antenna has been manufactured and tested on R & S

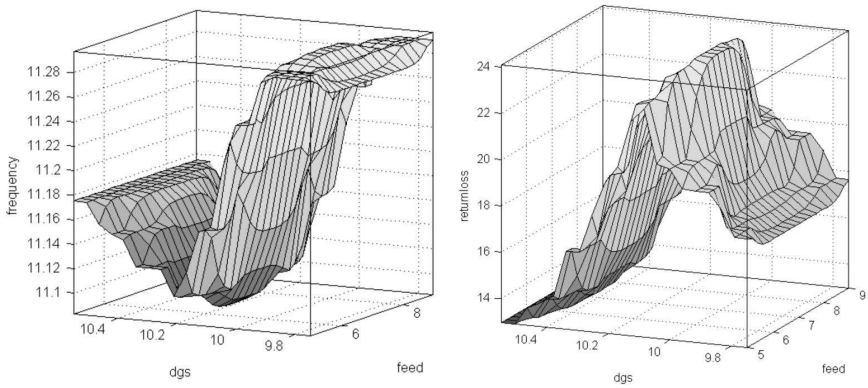

(a) (b)

Figure 2. Surface plot for the variation of feed location and position of defect with (a) frequency, (b) return loss.

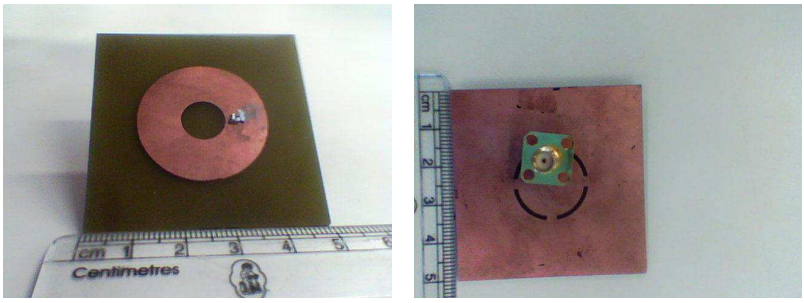

(a) (b)

Figure 3. Prototype of defected ground circular patch microstrip antenna. (a) Top view, (b) bottom view.

ZVL Vector network analyzer. The Figure 3 shows the top and bottom sides of the prototype of the proposed design.

4. SIMULATIONS AND MEASUREMENTS

In this section, the wide-band defected ground ring antenna is studied in detail. The antenna with and without DGS were simulated and verified by measurement results. Parameters such as return loss, input impedance, bandwidth, voltage standing wave ratio (VSWR) for the cases are measured and calculated. The simulated radiation pattern is also presented for the defected ground antenna structure.

When the ground plane for the proposed antenna is not defected and covers whole of the substrate, the simulated and measured values

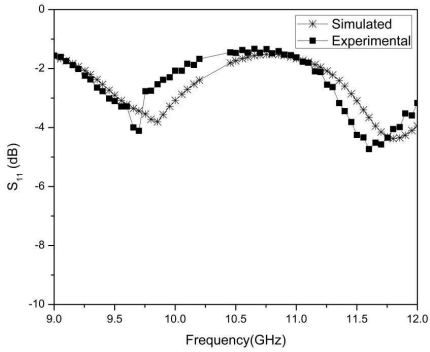

Figure 4. Simulated and experimental variation of reflection coefficient with frequency (without defect).

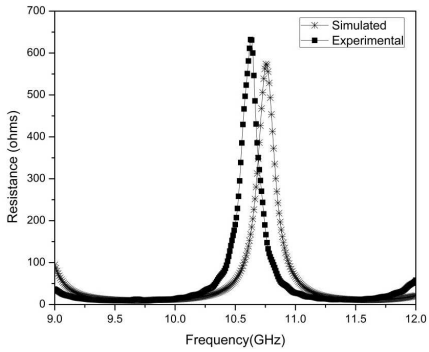

Figure 5. Simulated and experimental variation of impedance with frequency (without defect).

of reflection coefficient (S_{11}) are shown in Figure 4. The reflection coefficient is shown for the X-band. The antenna with no DGS resonates for TM_{32} mode at 11.70 GHz as calculated for $b = 3a$ from Eq. (6) above. The antenna is fed at 7 mm from the center. From the graph, it is clear that both simulated and experimental results are in good agreement. The simulated results shows TM_{32} resonating mode at 11.80 GHz with a return loss of 4.38 dB while the experimental value appears at 11.61 GHz with a return loss of 4.75 dB. It is obvious from the results that antenna does not show wideband characteristics. The variation of input impedance with frequency is shown in Figure 5. The input impedance is also about 15 ohms for both results. The low value of return loss and low impedance could be due to the unmatched feed point location. A proper choice of feed point location will result in good return loss and impedance matching at resonant frequency.

When the circular ring sector defect is introduced in the ground plane, the antenna shows a wide band in the X-band. The simulated and measured values of reflection coefficient are reported in Figure 6. From this figure, we can see that the antenna shows a wideband in the frequency range of 8–12 GHz with reduction of overall antenna size. Both experimental and simulated results are in good agreement. The antenna with DGS is again fed at 7 mm to excite the higher TM_{32} mode. The simulated results show that the antenna resonates at 11.29 GHz with a return loss of 25.95 dB. The simulated bandwidth is 1.33 GHz which is 11.78% about the center frequency of 11.29 GHz. The DGS antenna structure is then experimentally tested and the measured return loss is 20.51 dB at the frequency of 11.27 GHz. The return loss above 10 dB impedance bandwidth has a range of 1.2 GHz which is about 10.65% at the center frequency of 11.27 GHz.

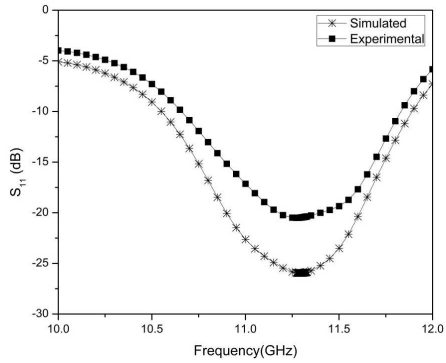

Figure 6. Simulated and experimental variation of reflection coefficient with frequency (with defect).

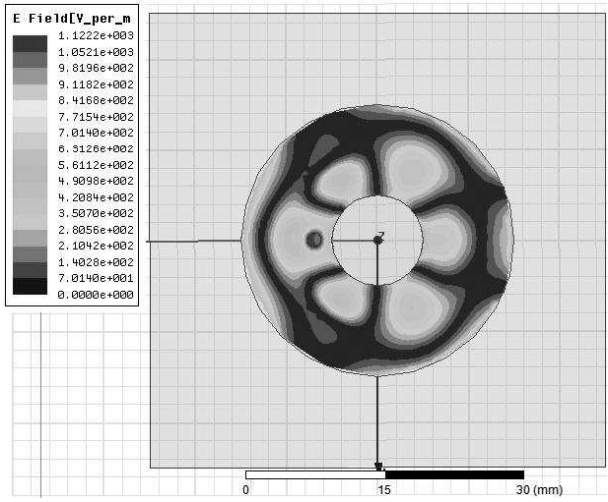

Figure 7. TM_{32} mode of the DGS patch at frequency 11.29 GHz (simulated).

When no defect was introduced in the antenna, its simulated TM_{32} mode was at 11.8 GHz. But due to the presence of defect in the ground plane, the same resonant mode is shifted towards the lower side at 11.29 GHz. Figure 7 shows the simulated TM_{32} resonant mode at the frequency 11.29 GHz. Thus the defect also reduces the overall size of the antenna.

The experimental and simulated input impedance is reported in Figure 8. It is evident from the results that experimental and simulated values are in good agreement. The DGS antenna shows a

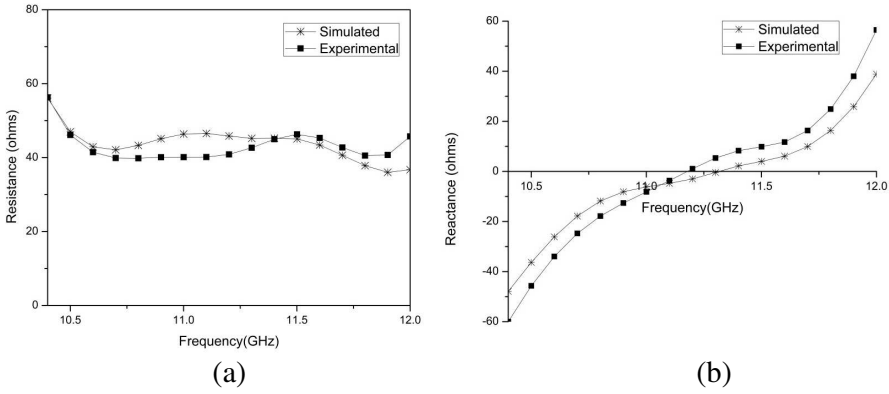

Figure 8. Simulated and experimental variation of impedance with frequency (with defect). (a) Real part, (b) imaginary part.

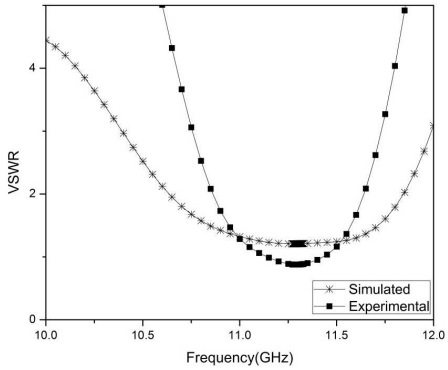

Figure 9. Simulated and experimental results for VSWR with frequency (with defect).

wide band in X-band and input impedance of nearly 50 ohm is achieved over the entire frequency range. The voltage standing wave ratio (VSWR) calculated from simulated and experimental results for the defected ground plane antenna is reported in Figure 9. The simulated bandwidth calculated is about 1.2 GHz while experimentally measured bandwidth is about 0.8 GHz for VSWR ≤ 2.

The simulated radiation patterns of E-plane and H-plane for the antenna structure with defected ground at frequency 11.29 GHz are shown in Figure 10. For E-plane (phi $= 0°$), the gain of the DGS antenna is 6.43 dB at $-4°$. The side lobe level is 2.75 dB below the main beam direction and the 3 dB beam width is 26.2° respectively.

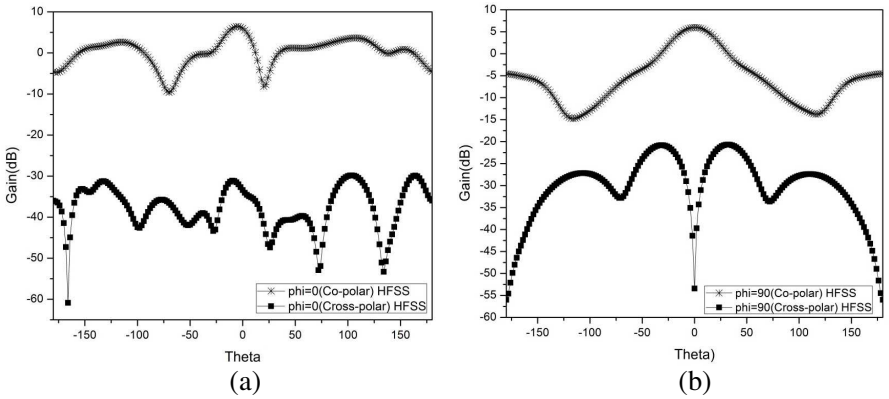

Figure 10. Radiation pattern (with defect) at frequency = 11.29 GHz. (a) E-plane (phi = 0°, co-polar & cross-polar), (b) H-plane (Phi = 90°, co-polar & cross-polar).

It is also clear from the graph that there is an isolation of 20.19 dB between co-polar and cross-polar radiations. The main beam shows a gain of 5.99 dB at 0° with side lobe level of −10.56 dB for H-plane (phi = 90°). The 3 dB beam width of about 60° is obtained for H-plane radiations. Also the cross-polar radiations are suppressed by 5.96 dB. The E-plane and H-plane radiation patterns show that a good antenna gain is achieved with suppressed cross-polar radiations.

It is apparent from all the results discussed above that the suggested DGS antenna shows an increased bandwidth with good impedance matching. The DGS also reduces the overall size of the antenna structure and suppresses the undesired cross-polar radiations from the main beam. In addition to this, the radiation properties of the defected ground antenna structure are also improved to a very good extent as compared to the normal antenna structure.

5. CONCLUSION

The low-profile circular ring DGS patch antenna with wide bandwidth and low level cross-polar radiations is presented in this paper. Measured results on fabricated antenna were used to confirm the simulation results. The propose DGS antenna with wide bandwidth was optimized using MATLAB FIS based on fuzzy decision-making. It has been observed that using the defected ground geometry and optimizing antenna parameter results in good impedance matching with high impedance bandwidth. The designed antenna operates in

X-band giving a wide impedance bandwidth. It is also observed that a good antenna gain and low level cross-polar radiations are obtained by introducing the circular ring sector defect in the ground plane. The measured results are in good agreement with the experimental results. At the end, an 11.78% bandwidth circular ring DGS patch antenna is designed, measured, and characterized in detail, which can be applied to modern wireless communication frequencies of X-band.

REFERENCES

1. He, W., R. Jin, and J. Geng, "E-shape patch with wideband and circular polarization for millimeterwave communication," *IEEE Trans. on Antennas and Propagation*, Vol. 50, No. 3, 893–895, 2008.
2. Bahl, J. and P. Bhartia, *Microstrip Antennas*, Artech House, Dedham, MA, 1980.
3. Gupta, K. C. and A. Benalla, (Editors), *Microstrip Antenna Design*, Artech House, Canton, MA, 1988.
4. James, J. R. and P. S. Hall, *Handbook of Microstrip Antennas*, IEE Electromagnetic Wave Series No. 28, Vols. 1, 2, Peter Peregrinus Ltd., London, 1989.
5. Bhartia, P., K. V. S. Rao, and R. S. Tomar, (Editors), *Millimeter-wave Microstrip and Printed Circuit Antennas*, Artech House, Canton, MA, 1991.
6. Pozar, D. M. and D. H. Schaubert (eds.), *Microstrip Antennas: The Analysis and Designof Microstrip Antennas and Arrays*, IEEE Press, New York, 1995.
7. Garg, R., P. Bhartia, I. Bahl, and A. Ittipiboon, *Microstrip Antenna Design Handbook*, Artech House, New York, 2001.
8. Maci, S. and G. BiffiGentilli, "Dual-frequency patch antennas," *IEEE Trans. on Antennas and Propagation Mag.*, Vol. 39, No. 6, 13–20, 1997.
9. Zulkifli, F. Y., E. T. Rahardjo, and D. Hartanto, "Radiation properties enhancement of triangular patch microstrip antenna array using hexagonal defected ground structure," *Progress In Electromagnetics Research M*, Vol. 5, 101–109, 2008.
10. Sharma, R., A. Kandwal, and S. K. Khah, "A novel multiband DGS antenna with enhanced bandwidth for wireless communication," *Mobile & Embedded Technology International Conference 2013*, 89–92, 2013.
11. Lim, J. S., S. Y. C. Jeong, D. Ahn, and S. Nam, "A technique

reducing the size of microwave amplifiers using spiral-shaped defected ground structure," *J. Korea Electromag. Eng.*, Vol. 14, No. 9, 904–911, Sep. 2003.

12. Kim, C. S., J. S. Park, and D. Ahn, "A novel 1-D periodic defected ground structure for planar circuits," *IEEE Microwave Guided Wave Lett.*, Vol. 10, No. 4, 131–133, Apr. 2000.
13. Lim, P. L. and K. M. Lum, "A novel bandpass filter design using E-shaped resonator and dual square-loop defected ground structure," *PIERS Proceedings*, 610–614, Kuala Lumpur, Malaysia, Mar. 27–30, 2012.
14. Zulkifli, F. Y., E. T. Rahardjo, and D. Hartanto, "Mutual coupling reduction using dumbbell defected ground structure for multiband microstrip antenna array," *Progress In Electromagnetics Research Letters*, Vol. 13, 29–40, 2010.
15. Zainud-Deen, S. H., M. E. S. Badr, E. Hassan, K. H. Awadalla, and H. A. Sharshar, "Microstrip antenna with defected ground plane structure as sensor for landmines detection," *Progress In Electromagnetics Research B*, Vol. 4, 27–39, 2008.
16. Lim, J. S., K. S. Kim, Y. T. Lee, D. Ahn, and S. Nam, "A spiral shaped defect ground structure for coplanar waveguide," *IEEE Microwave and Wireless Components Letters*, Vol. 12, No. 9, 330–332, 2009.
17. Weng, L. H., Y.-C. Guo, X.-W. Shi, and X.-Q. Chen, "An overview on defected ground structure," *Progress In Electromagnetics Research B*, Vol. 7, 173–189, 2008.
18. Hosseini, S. A., Z. Atlasbaf, and K. Forooraghi, "Two new loaded compact planar ultra-wideband antennas using defected ground structures," *Progress In Electromagnetics Research B*, Vol. 2, 165–176, 2008.
19. Li, L.-X., S.-S. Zhong, and M.-H. Chen, "Compact band-notched ultra-wideband antenna using defected ground structure," *Microwave and Optical Technology Letters*, Vol. 52, No. 2, 286–289, 2010.
20. Saad, A. A. R., E. E. M. Khaled, and D. A. Salem, "Wideband slotted planar antenna with defected ground structure," *PIERS Proceedings*, 1092–1097, Suzhou, China, Sep. 12–16, 2011.
21. Guha, D., M. Biswas, and Y. M. M. Antar, "Microstrip patch antenna with defected ground structure for cross polarization suppression," *IEEE Antennas Wireless Propag. Lett.*, Vol. 4, 455–458, 2005.
22. Kumar, C. and D. Guha, "New defected ground structures

(DGSs) to reduce cross-polarized radiation of circular microstrip antennas," *IEEE Applied Electromagnetic Conf. AEMC 2009*, 1–4, Kolkata, India, 2009, DOI: 10.1109/AEMC.2009.5430671.

23. Guha, D., C. Kumar, and S. Pal, "Improved cross-polarization characteristics of circular microstrip antenna employing arc-shaped defected groundstructure (DGS)," *IEEE Antennas Wireless Propag. Lett.*, Vol. 8, 1367–1369, 2009.
24. Salehi, M. and A. Tavakoli, "A novel low mutual coupling microstrip antenna array design using defected ground structure," *Int. J. Electron Commun.*, Vol. 60, 718–723, 2006.
25. Guha, D., S. Biswas, and C. Kumar, "Annular ring shaped dgs to reduce mutual coupling between two microstrip patches," *IEEE Applied Electromagnetic Conf. AEMC 2009*, 1–3, Kolkata, India, 2009, DOI: 10.1109/AEMC.2009.5430663.
26. Guha, D., S. Biswas, T. Joseph, and M. T. Sebastian, "Defected ground structure to reduce mutual coupling between cylindrical dielectric resonator antennas," *Electronic Lett.*, Vol. 44, No. 14, 836–837, Jul. 2008.
27. Moghadas, H., A. Tavakoli, and M. Salehi, "Elimination of scan blindness in microstrip scanning array antennas using defected ground structure," *Int. J. Electron. Commun.*, Vol. 62, 155–158, 2008.
28. Ostadzadeh, S. R., M. Soleimani, and M. Tayarani, "A fuzzy model for computing input impedance of two coupled dipole antennas in echelon form," *Progress In Electromagnetics Research*, Vol. 78, 265–283, 2008.
29. Ostadzadeh, S. R., M. Tayarani, and M. Soleimani, "A fuzzy model for computing back scattering respose from linearly loaded dipole antenna in the frequency domain," *Progress In Electromagnetics Research*, Vol. 86, 229–242, 2008.
30. Guney, K. and N. Sarikaya, "Comparison of Mamdani and Sugeno fuzzy inference system models for resonant frequency calculation of rectangular microstrip antennas," *Progress In Electromagnetics Research B*, Vol. 12, 81–104, 2009.
31. PDF Documents on *Fuzzy Logic Toolbox of Matlab 7.10.0*, http://www.mathworks.com/.